Electronic Supplementary Material (ESI) for Journal of Materials Chemistry A.

Supporting Information

Confining Single Pt Atom from Pt Clusters on Multi-Armed CdS for Enhanced Photocatalytic Hydrogen Evolution

Xiangyu Lu,[a,#] Aomei Tong,[b,#] Dian Luo,[a,#] Fan Jiang, [a] Jieding Wei, [a] Yucheng Huang, [a,*] Zheng Jiang,[c] Zhou Lu[b,*] and Yonghong Ni [a,*]

[#] Equal contribution for this work.

[a] College of Chemistry and Materials Science, Key Laboratory of Functional Molecular Solids, Ministry of Education, Anhui Laboratory of Molecule-Based Materials, Anhui Normal University, 189 Jiuhua Southern Road, Wuhu, 241002, PR. China. Email: huangyc@mail.ahnu.edu.cn (Y.C. Huang); niyh@mail.ahnu.edu.cn (Y.H. Ni)

[b] School of Physics and Electronic Information, Anhui Normal University, 189 Jiuhua Southern Road, Wuhu, 241002, PR. China. Email: zhoulu@mail.ahnu.edu.cn (Z. Lu)

[c]Shanghai Synchrotron Radiation Facility, Zhangjiang Lab, Shanghai Advanced Research Institute, Chinese Academy of Science, Shanghai, P. R. China

Experimental section

Reagents. chloroplatinic acid, L-reduced glutathione, sodium tetrahydridoborate were purchased from Sinopharm Chemical Reagent Co., Ltd. (Shanghai, China). $CdCl_2·2.5H_2O$, thiourea, dodecylthiol and ethylenediamine (EDA) were brought from Macklin. Deionized (DI) water with a resistivity of 18.25 MΩ·cm was used in all experiments. All the reagents in this experiment were analytical grade and used as received without further purification.

Synthesis of $Pt_5(GS)_{10}$ clusters. $Pt_5(GS)_{10}$ clusters were synthesized according to a reported method with some modifications. [1] In a typical synthesis, $H_2PtCl_6·6H_2O$ (0.20 mmol) and L-reduced glutathione (GSH) (0.75 mmol) were dissolved in 6 mL of H_2O and stirred for 2 h at 0 °C; Then, 2.0 mL of the freshly prepared ice cold $NaBH_4$ (1.5 mmol) aqueous solution was added under vigorous stirring. After five hours, excess methanol was added to the solution, and the obtained yellow precipitate was collected by centrifugation and washed repeatedly with methanol, finally dried at 60 °C under vacuum overnight.

Synthesis of multi-armed CdS nanorods. Multi-armed CdS nanorods were prepared according to the literature with some modifications.[2] Typically, $CdCl_2·2.5H_2O$ (0.074g, 0.4mmol), thiourea (0.051g,0.67mmol), dodecylthiol (8 g) and EDA (3 g) were put into a Teflon-lined stainless-steel autoclave with a volume of 25 mL. The autoclave was then filled with toluene up to 70% of its volume and maintained at 160 °C for 40 h. After cooling to room temperature naturally, the product was collected by centrifugation, washed with toluene and anhydrous ethanol several times, followed by drying at 60 °C in vacuum oven for 24 h. The powder was obtained for further use and characterization.

Synthesis of Pt_5/CdS. Typically, a calculated amount of $Pt_5(GS)_{10}$ clusters was dissolved in 2.0 mL of distilled water, and then added dropwise to a suspension containing 20 mg CdS nanorods. After stirring at room temperature for 3 h, $Pt_5(GS)_{10}/CdS$ composites were collected by evaporating solvent under vacuum, and dried overnight at 60 °C. Finally, the obtained powder was calcined in Ar atmosphere at a heating rate of 5 °C/min and maintained at 300 °C for 1 h. After cooling to room temperature naturally, the Pt_5/CdS catalyst was obtained.

Characterizations. The phases and chemical compositions of the samples were analyzed on a Bruker D8 X-Ray Diffractometer with Cu Kα radiation (λ = 1.5406 Å). Transmission electron microscopy (TEM) images of the products were taken on a Hitachi HT7700 transmission electron microscope at an acceleration voltage of 120 kV, using the carbon-coated copper grid. The lattice fringe and fast Fourier transform (FFT) image were obtained by high resolution transmission (HRTEM) in Tecnai G2 (Thermo Fisher Scientific). The high-angle annular dark-field scanning transmission electron microscopy (HAADF-STEM) images and STEM-EDX elemental mappings were collected on FEI Talos F200X (Thermo Fisher Scientific). The valence state of the element was detected by X-ray photoelectron spectroscopy, which were carried out on an ESCALAB 250Xi instrument with a monochromatic Al Kα (hν = 1486.6 eV) with the X-ray beam spot of 500 μm and the transmittance of 30 eV. The FT-IR spectrum was recorded from KBr pellets in the range of 4000–400 cm^{-1} on a Prestige-21 SHIMADZU FT-IR spectrometer. Steady state fluorescence spectra were conducted on FLSP 920 (Edinburgh Instruments, UK). All electrochemical measurements were performed on a CHI660E electrochemical station (Chenhua, Shanghai). Electrochemical impedance spectroscopy (EIS) was conducted at the open circuit potential over the frequency range from 10^{-2} to 10^5 Hz with AC signals of amplitude of 5 mV. The measurements were carried out in a three-electrode system with the graphite rod as the counter electrode and an Ag/AgCl as the reference electrode at room temperature in 0.5 M Na_2SO_4 solution. The working electrodes were prepared as follows: 2 mg of catalysts were firstly dispersed into a mixed solvent of 2 mL ethanol and 10 μL Nafion under the ultrasound assistance; and then, the formed slurry was coated on Ni foam with the size of 1 × 1 cm^2. The photocurrent measurements were performed on electrochemical station (CHI660E, Shanghai Chenhua Limited, China) with simulated solar light irradiation. Here, the indium tin oxide (ITO) glass was used as the substrate for preparing the working electrode. The photocurrent signals of the samples were measured under chopped light. The measurements were also carried out on a conventional three-electrode cell in 0.5 M Na_2SO_4 solution. The XAFS Spectroscopy measurements were performed at the beamline BL14W1 of Shanghai Synchrotron Radiation Facility (SSRF). The electron beam energy of the storage ring was 3.5 GeV with a maximum stored current of 300 mA.

Ultrafast transient absorption (TA) spectroscopy characterizations. The femtosecond transient absorption (TA) spectra were acquired with a typical transmission pump-probe (UV/vis pump-broadband supercontinuum probe) instrument. A Ti:sapphaire regenerative amplifier (Spitfire Ace, Spectra Physics, Inc.) produced laser pulses (6 mJ, 1 kHz) with a pulse width of 80 fs and center wavelength at 800 nm. The laser output was then split into several beams, one of which was used to generate wavelength-tunable light serving as the pump laser for TAS via a downstream optical parametric amplifier (TOPAS-Prime). In current work, 400 nm was chosen as the center wavelength of the TOPAS-Prime output. The pump laser was attenuated to 160 nJ and chopped with a 500 Hz mechanical chopper. Another laser beam propagated through an optical delay line (0-8 ns) and was then focused into a CaF_2 crystal to produce white light continuum, which serves as the probe light in the fs-TA. The pump and probe light overlap in the sample cell with an optical path of 2 mm. All experiments were conducted at room temperature. The CdS NRs and Pt_5/CdS heterostructures were both dispersed in ethylene glycol (0.22 mg/mL).

Computational methods. All the calculations were based on density functional theory (DFT) and implemented in the Vienna ab initio simulation package (VASP).[3] The ion-electron interactions were described with the projector-augmented wave (PAW) method.[4] Exchange-correlation potentials were expressed by the Perdew−Burke−Ernzerhof (PBE) form with the generalized gradient approximation (GGA).[5] An energy cutoff of 450 eV was used for the plane-wave basis set. The residual energy and force convergence criterion was set to 10^{-5} eV and 0.02 eV $Å^{-1}$, respectively. A vacuum space of 20 Å was applied to avoid interactions between two periodic units. In the geometry optimization and static self-consistent calculations, the k-point meshes of 2×2×1 generated by the Monkhorst-Pack Scheme were used. [6]

To calculate the hydrogen-adsorption Gibbs free energy (ΔG_{H*}), an interfacial model was constructed where we put a Pt-S_4 on the supercell of 4×4×1 CdS (11-20) surface, 4×4×2 CdS (0001) surface and 4×4×1.5 CdS (10-10) surface. To cancel out the artificial electric field due to the net electric dipole moment that arises in polar surface calculations, a dipole correction was also used. According to the methodology developed by Nørskov et al.,[7] the chemical potential of $H^+ + e^-$ is equal to that of 1/2 H_2 at standard condition (pH = 0, P_{H2} = 1 bar, T = 298 K). ΔG_{H*} was considered to characterize the hydrogen evolution reaction (HER) activity:

$$\Delta G_{H*} = \Delta E_{H*} + \Delta E - T\Delta S$$

Where ΔE_{H*} is the difference of hydrogen adsorption energy, which can be calculated using the formula of $\Delta E_{H*} = E_{T+H*} - E_T - 1/2\ E_{H2}$. Here E_{T+H*}, E_T and 1/2 E_{H2} represent the total energies of Pt_5/CdS with one hydrogen atom adsorbed on the heterostructure, Pt_5/CdS and H_2 molecule, respectively. ΔE is the difference in zero-point energy (ZPE) between the adsorbed H* and molecular H_2 in gas phase, which can be obtained via vibrational frequency calculations; T is the temperature (set as 298.15 K), and ΔS is the difference in entropy. Due to the slight influence on the ΔG_{H*}, the solvation effect is not taken into account in this work.[8]

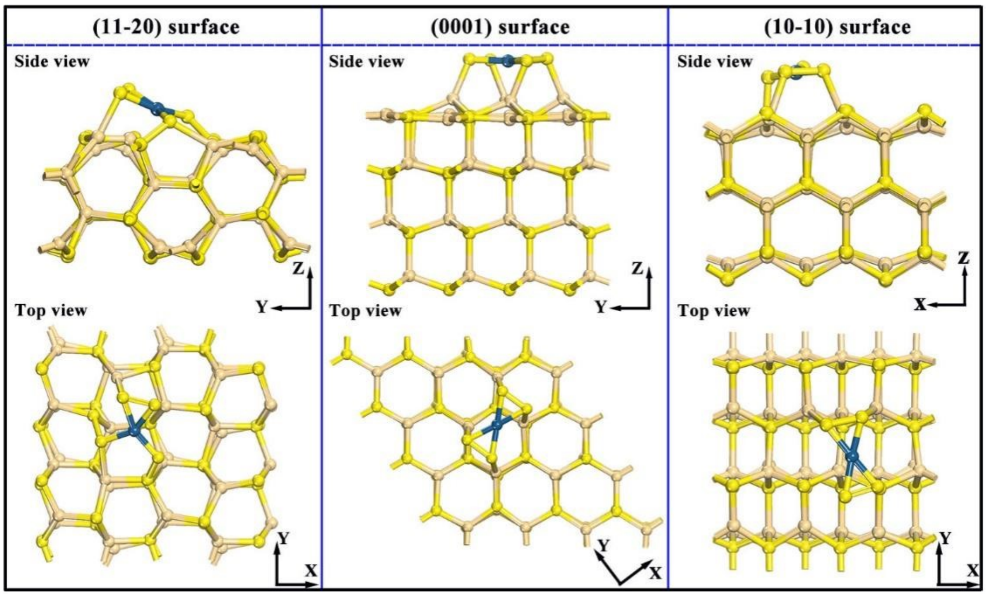

The supercells of 4×4×1 CdS (11-20), 4×4×2 CdS (0001) and 4×4×1.5 CdS (10-10) surfaces.

Photocatalytic hydrogen production measurements. The photocatalytic H_2 evolution experiments were performed in a 100 mL reaction cell connected to a gas-closed glass vacuum system. Typically, 5 mg of the photocatalyst was suspended in a mixed solvent containing 2 mL of triethanolamine (TEOA) and 8 mL of H_2O. A 300 W Xe lamp with a 400 nm cutoff filter and full solar spectral band reflector was used as the light source. During the photocatalysis, the reaction system was vigorously stirred with a magnetic stirrer, and the reaction temperature was controlled at 6 °C by circulating cooling water. The amount of hydrogen produced from the photocatalytic reaction was sampled and quantified by gas chromatography with Ar as the carrier gas.

References:

1. X. K. Wan, H. B. Wu, B. Y. Guan, D.Y. Luan, X. W. Lou, *Adv. Mater*. **2019**, 1901349.
2. F. Gao, Q.Y. Lu, S.H. Xie, D.Y. Zhao, *Adv. Mater.* **2002**, *14*, 1537-1540.
3. G. Kresse, J. Furthmüller, *Phys. Rev. B.* **1996,** *54*, 11169.
4. P. E. Blöchl, *Phys. Rev. B.* **1994,** *50*, 17953.
5. J. P. Perdew, K, Burke, M, Ernzerhof, *Phys. Rev. Lett.* **1996,** *77*, 3865.
6. H. J. Monkhorst, J. D. Pack, *Phys. Rev. B.* **1976**, *13,* 5188–5192.
7. K. Mathew, R. Sundararaman, K. Letchworth-Weaver, T. A. Arias, R. G. Hennig, *J. Chem. Phys.* **2014,** *140,* 084106.
8. Y. Ping, G. Galli, *The J. Phys. Chem. C.* **2014,** *118*, 6019-6028.

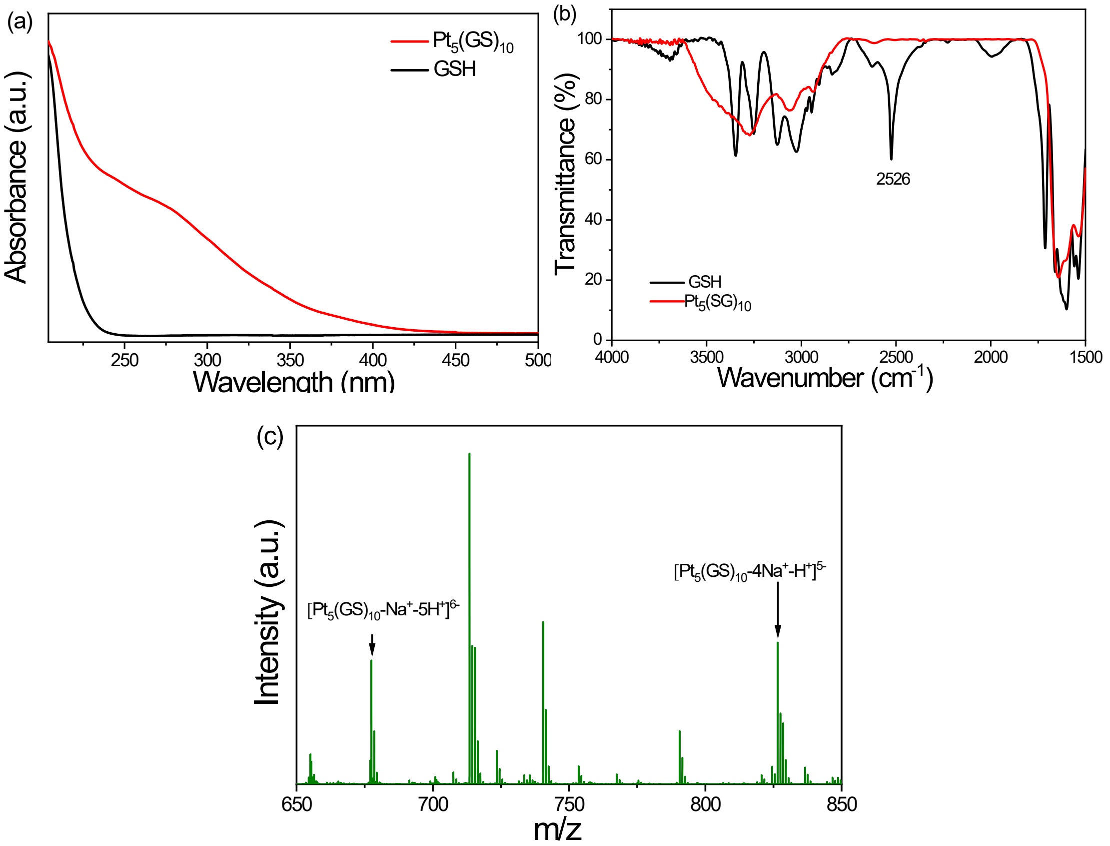

Figure S1. (a) UV-Vis absorption and (b) FTIR spectra of the $Pt_5(GS)_{10}$ clusters and pure GSH and (c) ESI-MS profile of the product. The mass spectrum shows that the product consists of $Pt_5(GS)_{10}$

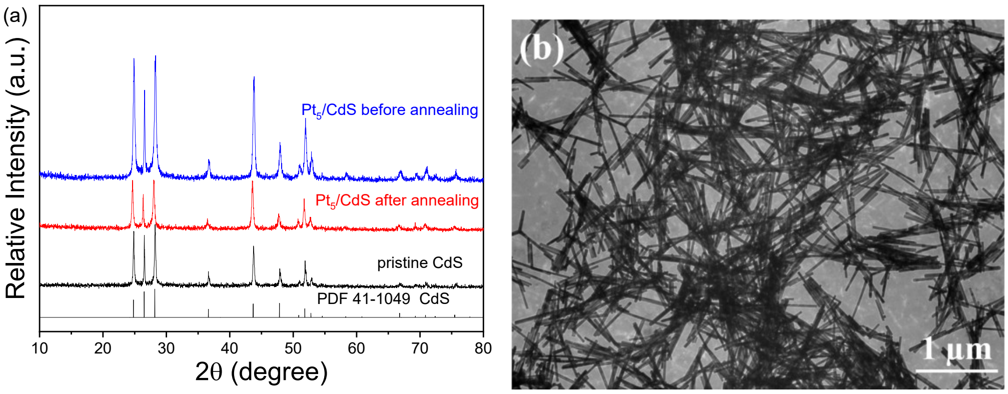

Figure S2. (a) XRD patterns of pristine CdS, Pt_5/CdS before and after annealing; and (b) TEM image of CdS.

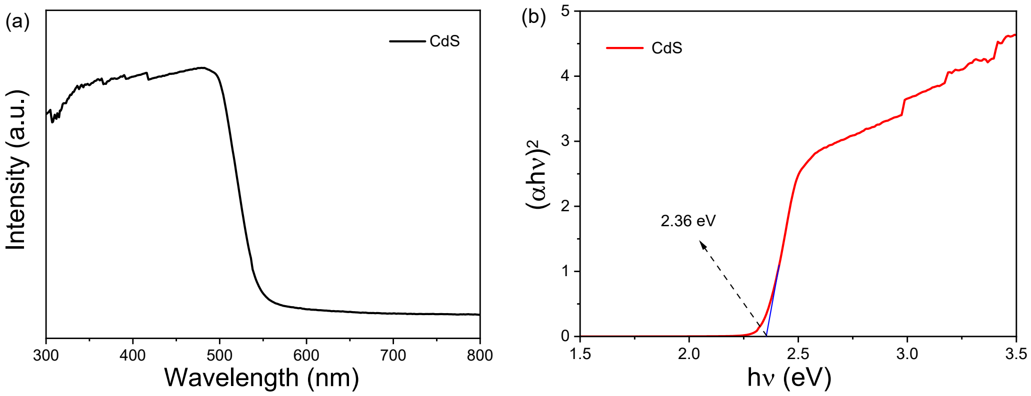

Figure S3. (a) UV/Vis diffuse reflection spectrum and (b) the corresponding Tauc plot of CdS.

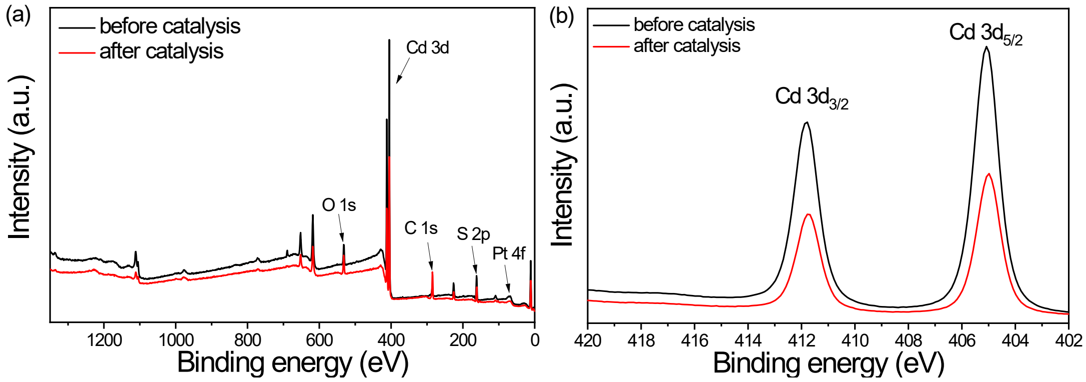

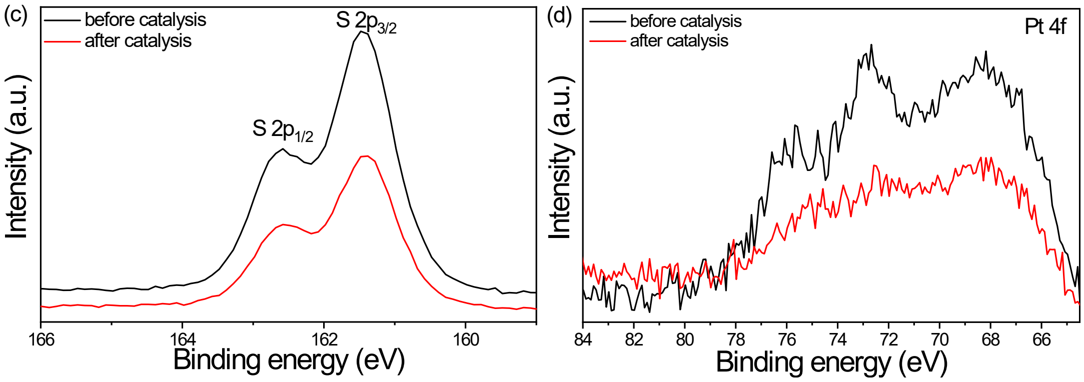

Figure S4. XPS analyses of the as-obtained Pt_5/CdS before and after photocatalysis: (a) survey spectra, (b) Cd 3d, (c) S 2p and (d) Pt 4f.

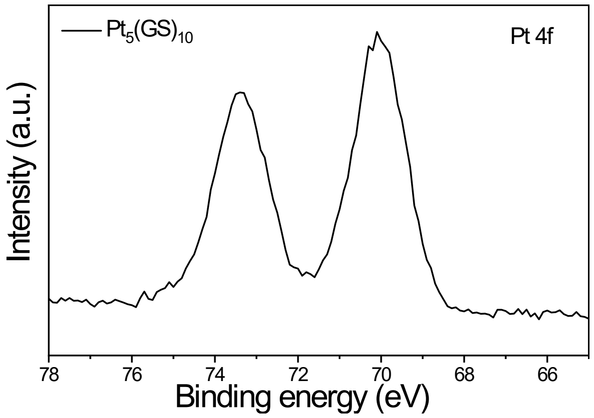

Figure S5. Pt 4f XPS spectrum of $Pt_5(GS)_{10}$.

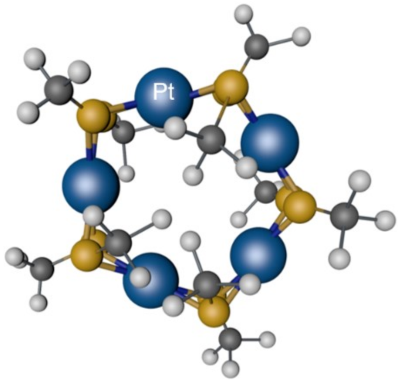

Figure S6. The molecular structure of $Pt_5(GS)_{10}$.

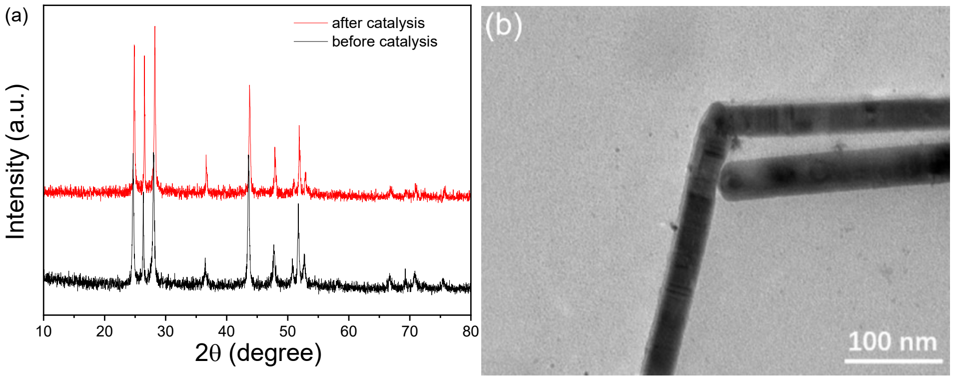

Figure S7. (a) XRD pattern and (b) TEM image of the Pt_5/CdS photocatalyst after durability tests.

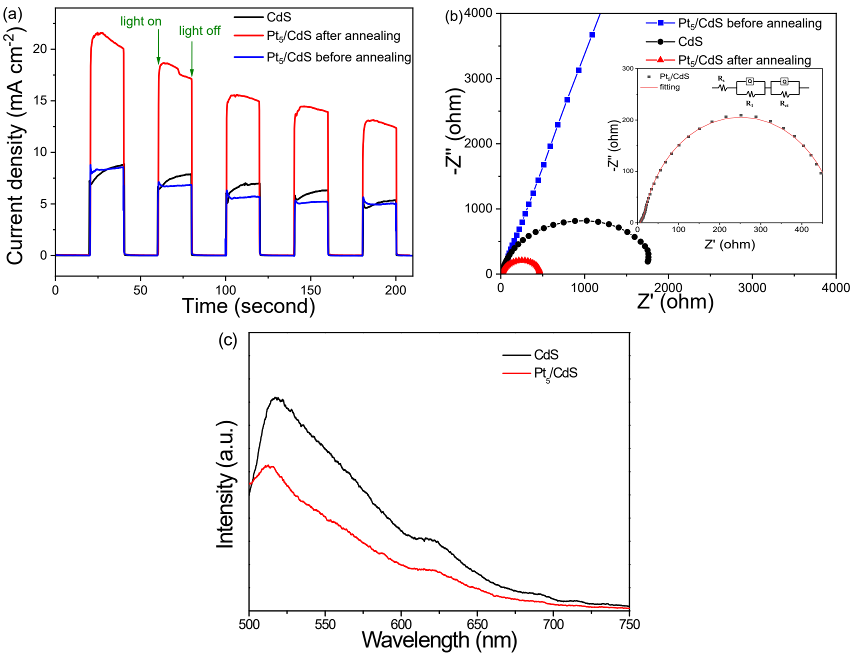

Figure S8. (a) The photocurrent responses, (b) Nyquist plots and (c) PL emission spectra of Pt_5/CdS and CdS.

Table S1. Mass percentages of Cd, S and Pt elements in Pt_5/CdS based on ICP-MS technology.

Element	Mass percentage /%
Cd	68.15
Pt	0.10
S	10.61

Table S2. Structural parameters of Pt_5/CdS extracted from the EXAFS fitting ($S_0^2 = 0.80$).

Path	CN	R(Å)	$\sigma^2(10^{-3}\text{Å}^2)$	ΔE_0(eV)	R factor
Pt-S	4.0±0.2	2.31±0.2	4.3±0.4	4.8±0.4	0.02

S_0^2 is the amplitude reduction factor; CN is the coordination number; R is interatomic distance (the bond length between central atoms and surrounding coordination atoms); σ^2 is Debye-Waller factor (a measure of thermal and static disorder in absorber-scatterer distances); ΔE_0 is edge-energy shift (the difference between the zero kinetic energy value of the sample and that of the theoretical model). R factor is used to value the goodness of the fitting.

Table S3. Comparison of photocatalytic H_2 production performances of Pt_5/CdS with some Pt-based photocatalysts reported in the literatures.

Catalysts	Reaction Conditions	Hydrogen generation rate (μmol h^{-1} g^{-1})	Light Source	Refs.
Pt$_5$/CdS	TEOA	12972	λ > 400 nm	This work
0.5% Pt-S doped H-TiO$_2$	25%CH$_3$OH	258	AM1.5	*J. Am. Chem. Soc.*, **2013**, *135,* 17831.
1%Pt/TiO$_2$	10% CH$_3$OH	4000	Xe lamp 200W	*Nat. Commun.***2015**, *6*, 5881.
0.5 wt% Pt/CdS	20 vol% lactic acid	3650	λ > 420 nm	Nano Today. **2021***37*, 101080.
Al-TCPP-0.1Pt	5 %TEOA	129	λ > 380 nm	*Adv. Mater.* **2018**, *30*, 1705112.
4wt%Pt/CdS NP/Cd NSs	Na$_2$S(0.35M)/Na$_2$SO$_3$(0.25 M)	16800	λ > 420 nm	*Adv. Energy Mater.***2016**, *6*, 1501241.
Au-Pt-CdS	Na$_2$S/Na$_2$SO$_3$	778	λ > 420 nm	*Adv. Funct. Mater.***2016**, *26*, 6076-6083.
2.87%Pt@UiO-66-NH$_2$	10 %TEOA	257.38	λ > 380 nm	*Angew. Chem. Int. Ed.* **2016**, *55,* 9389.
0.16%Pt/g-C$_3$N$_4$	10 % TEOA	6360	300 W Xe lamp	*Adv. Mater.* **2016**, *28*, 2427.
0.6%Pt/TiO$_2$	50% CH3OH	10000	AM 1.5	*Science*, **2011**, 331, 746.
HNMT-Ir/Pt	TEOA	201	λ > 400 nm	*Angew. Chem. Int. Ed.* **2018**, *57*, 3493-3498.
3%Pt/CTF-HUST-2	10 %TEOA	2647	λ > 420 nm	*Angew. Chem. Int. Ed.* **2017**, *56*, 14149.
1%PtO/TiO$_2$	CH$_3$OH	4400	Xe lamp, 300 W	*Nat. Commun.***2015**, *6*, 5881.
0.16%Pt/g-C$_3$N$_4$	TEOA	6360	Xe lamp, 300 W	*Adv. Mater.***2016**, *28*, 2427.
TiO$_2$/C$_3$N$_4$	TEOA，1wt% Pt	770	AM1.5	*Appl. Catal. B.***2016**, *191*, 130-137
1%Pt-Sub-10nm rutile TiO$_2$ nanoparticles	CH$_3$OH	1954	AM1.5	*Nat. Commun.***2015**, *6*, 5881.
Pt1@CN@CuS	CH$_3$OH	508.8	λ > 420 nm	*Angew. Chem. Int. Ed.***2020**, *59*, 2 – 9

Table S4. The solution resistance (R_s), charge transport resistance within the electrode (R_{ct}) and charge transfer resistance at the solid/electrolyte interface (R_1) of the Pt_5/CdS /NF electrode.

R/Ω	$\mathbf{R_s}$	$\mathbf{R_1}$	$\mathbf{R_{ct}}$
Pt_5/CdS	6.64	469.8	9.30

Table S5. Kinetic parameters of transient absorption decays of CdS and Pd_5/CdS under 400-nm excitation.

Sample	τ_{rise} *(ps)*	τ_1 *(ps)*	τ_2 *(ps)*	τ_3 *(ns)*
CdS	0.4	8 ± 1 (29.4%)	96 ± 5 (53.0%)	1.1 ± 0.2 (17.6%)
Pd_5/CdS	0.1	6 ± 1 (28.7%)	45 ± 2 (55.6%)	1.4 ± 0.2 (15.7%)